



# THE UNIVERSITY *of* EDINBURGH

## Edinburgh Research Explorer

### **Co-optimization of demand response and interruptible load reserve offers for a price-making major consumer**

**Citation for published version:**

Habibian, M, Zakeri, G, Downward, A, Anjos, MF & Ferris, M 2018, 'Co-optimization of demand response and interruptible load reserve offers for a price-making major consumer', *Energy Systems*.  
<https://doi.org/10.1007/s12667-018-0312-x>

**Digital Object Identifier (DOI):**

[10.1007/s12667-018-0312-x](https://doi.org/10.1007/s12667-018-0312-x)

**Link:**

[Link to publication record in Edinburgh Research Explorer](#)

**Document Version:**

Peer reviewed version

**Published In:**

Energy Systems

**General rights**

Copyright for the publications made accessible via the Edinburgh Research Explorer is retained by the author(s) and / or other copyright owners and it is a condition of accessing these publications that users recognise and abide by the legal requirements associated with these rights.

**Take down policy**

The University of Edinburgh has made every reasonable effort to ensure that Edinburgh Research Explorer content complies with UK legislation. If you believe that the public display of this file breaches copyright please contact [openaccess@ed.ac.uk](mailto:openaccess@ed.ac.uk) providing details, and we will remove access to the work immediately and investigate your claim.



# Co-optimization of Demand Response and Interruptible Load Reserve Offers for a Price-Making Major Consumer

Mahbubeh Habibian<sup>1</sup> · Golbon Zakeri<sup>1</sup> · Anthony Downward<sup>1</sup> · Miguel F. Anjos<sup>2</sup> · Michael Ferris<sup>3</sup>

the date of receipt and acceptance should be inserted later

**Abstract** We study demand-side participation in an electricity market for an industrial consumer of electricity, with some flexibility to reduce demand, and capable of offering interruptible load reserve. Our consumer is a price maker, and the impact of its actions in the market is modelled via a bi-level optimization problem. We have extended a standard model for optimal strategic consumption, to the case where reserve offer curves need to be optimized simultaneously with consumption curves; our models provide intuition into this interaction. Furthermore, we provide tailor-made solution strategies for the resulting problems under uncertainty, and report numerical results of our implementation on instances over the full New Zealand network yielding a realistic and large problem set.

**Keywords** Demand response · Bi-level optimization · Decomposition methods · Integer programming · Stochastic optimization

## 1 Introduction

Absence of demand response is considered a significant market failure in electricity markets [1]. This absence prevents curtailment of demand in response to supply scarcity which is a necessity for any well functioning competitive market, particularly when power supply is unreliable. Electricity markets have started to enable consumers to be active participants, who can provide elasticity, and contribute to efficiency. In addition to improving reliability of the electricity sector, demand response can enable deferral of expensive generation and transmission investments, and can also result in better integration of renewable generation technologies. Since distributed electricity technologies have started to become cost-effective, (e.g. solar PVs and battery storage), there has been a growing body of work on household demand response [2–7]. A number of authors have discussed demand response in restricted formats, e.g. [8–10] and have examined its potential and limitations [11–13]. However, there has been less research on full-scale models for large consumers of electricity with strategic bidding schemes.

---

M. Habibian  
E-mail: mhab735@aucklanduni.ac.nz

G. Zakeri  
E-mail: g.zakei@auckland.ac.nz

A. Downward  
E-mail: a.downward@auckland.ac.nz

M. F. Anjos  
E-mail: miguel-f.anjos@polymtl.ca

M. Ferris  
E-mail: ferris@cs.wisc.edu

<sup>1</sup>University of Auckland

<sup>2</sup>Polytechnique Montreal

<sup>3</sup>University of Wisconsin

Major industrial users of electricity form an important group that can provide substantial demand response in any electricity market. In the US, approximately 30% of electricity is consumed by industrial consumers [14], while this figure is roughly 35% in New Zealand [15]. In this paper, we model a price-making consumer, who is capable of affecting the price of electricity through reducing their consumption. Our focus is on developing an effective methodology for the solution of the resulting models to provide decision making tools, under uncertainty, for a large consumer of electricity in a realistic market setting. Our models and tools will shed light on the behaviour of such large consumers. Our models also can be of use for the market regulators for understanding the policy implications of enabling dispatchable demand.

In a number of electricity markets (Singapore, Mid-continent ISO, New Zealand, etc.), reserve (in varying forms), and energy are co-optimized in the same market clearing auction. Such markets accept the traditional supply offers (offer stacks) and demand bids for energy, and in addition they accept reserve supply offers (reserve stacks) that can be offered by generators or large consumers capable of providing reserves. The reserves are typically fast responding reserves in the form of tail-water depressed (offered by hydro generators), or interruptible load reserves (ILR) that is offered by major consumers. The ability of large consumers to submit ILR offer stacks gives rise to an challenging optimization problem, which we tackle in this work. Here, the major consumer not only decides on an optimal demand bid curve, but also simultaneously optimizes a reserve offer stack, both of which are submitted to the market. The stack nature of these curves provides some flexibility to cope with uncertainty, which is a cornerstone feature of our application given the make up of any electricity market, and volatility in prices.

In order to address the strategic bidding and offering of the major consumer, we present a bi-level optimization problem that maximizes the consumer's profit (the upper level problem), given the co-optimized optimal power flow problem (OPF) as the lower level problem. We later lay out the mathematical model of the co-optimized OPF in subsection 2.1. While a basic formulation of the stochastic bi-level program for optimal energy consumption of a large consumer in an electricity market has been offered in [16], no efficient methodology to solve this problem has been discovered prior to the current paper. Furthermore, we extend the model offered in [16], to include the optimal construction of a reserve offer stack in conjunction with optimizing the demand bid curve. This co-optimization makes the problem even more difficult to solve, and we develop tailor-made solutions that take advantage of the problem structure. We also report on numerical results that demonstrate the effectiveness of our methodology. We show that our model is important since the resulting consumer behaviour can lead to significant efficiency increases.

Similar models to ours have been introduced, however, our work is new and fundamentally different in several ways.

1. Our model allows for strategic interaction of the large consumer with the market in *both* demand response and reserve offers. Most papers to date ( see e.g. [17–19]) either ignore the capability of the consumer to offer reserves, or assume the consumer provides all reserves at price zero. We illustrate the importance of this feature of our model and the effects it has on the consumer's consumption strategy in subsection 2.1.
2. All existing literature uses the standard reformulations of complementarity conditions to Mixed Integer Programs (MIPs). In contrast, we develop and investigate tailor-made solution approaches for the resulting bi-level optimization problems that make it possible to solve these problems on a real electricity network consisting of several hundred nodes.
3. We offer a sampling methodology, from historical information, to make the solution procedure fully implementable for a large consumer in a real world electricity market and report on the results.

Moreover, our paper extends the work of Cleland et al. [20] to deliver admissible optimal policies in the form of a demand curve and corresponding reserve stack (whereas the policies defined in [20] do not yield a bid curve for energy). Also, unlike Cleland et al. [20], we do not confine our solution to a priori discretized set; we instead optimize over the continuum of quantity and price. An example highlighting the differences of our work to the previous work is supplied in section 2.2.

We lay out the paper as follows. In section 2, we present our price-making consumer's profit maximizing bi-level optimization model. We discuss the impacts of strategic co-optimization and the advantages of our proposed model in two illustrative examples. In subsection 2.2 we probe the extent of our contribution to the literature, with comparing our method with the model presented

in [20,21]. In order to be able to solve our model to global optimality, in section 3, we discuss the standard reformulation methods that may be used to reformulate our bi-level model to a MIP. In subsection 3.1 we present an innovative alternate method to reformulate our bi-level optimization problem. To address decision making under uncertainty, in section 4, we proceed to the stochastic version of our model where the major consumer submits monotone interruptible load reserve (ILR) offer and demand bid curves. In section 5 we compare the solution times of our proposed decomposition method with the standard MIP reformulation and present our computational results for a large electricity consumer in the New Zealand Electricity Market (NZEM). Section 6 concludes the paper.

## 2 Price-making major consumer

Recent changes in many de-regulated electricity markets have allowed for demand-side bids to be accepted into the spot market, enabling consumers to reflect their real-time elasticity to energy prices. Major consumers have large enough loads that reducing their consumption could have a noticeable impact on the market price. Due to the hockey stick nature of electricity offer stacks (as we approach system capacity the prices rise sharply), responding to price in high price periods not only reduces the consumption of high priced electricity, but also leads to a decrease in spot prices. As an aside, demand response can potentially reduce generation from the least efficient and oftentimes most polluting peaking plants. Our model considers a strategic consumer who takes account of the influence of its actions on the prices of energy (and reserve). Due to the prices for energy and reserve being interrelated, this model enables the price-making consumer to alleviate any pressure on reserve and thereby reduce the price of electricity. In this section we explore the characteristics of strategic behaviour for a major consumer. We first lay out our bi-level formulation. In addition, using this model, we present an example over a small network, and report on a sensitivity analysis of a strategic consumer's bid in a deterministic setting. This example is followed by the discussion of the impacts of strategic co-optimization on the consumer and the market. The second part of this section compares the method introduced in this paper with the most recent and relevant literature on large-scale co-optimized demand response in [21]. We will illustrate the advantages of our methodology over this existing method.

### 2.1 Offering reserve matters

In co-optimized markets such as the NZEM, in addition to the frequency keeping reserve that is partially co-optimized, the OPF problem also ensures that sufficient reserves are procured against the event of the sudden shutdown of a large source of energy supply (referred to as  $N-1$  contingency reserve). In this paper we use the term reserve for the contingency reserve and not the frequency keeping reserve (additional examples of different terminology throughout the world are presented in [22] and [23]). First, we present the co-optimized OPF problem (called [D-LP]). For this section, we use the following notation to formulate our model:

$f_{ij}$	The flow between node $i$ and $j$ .
$K_{ij}$	The line capacity in arc $ij$ .
$r_e$	The reserve level required in zone $e$ .
$V_n$	The minimum amount of difference between ILR and consumption, at node $n$ . It denotes the level of consumption that can not be interrupted.
$B_n$	The fraction of generation allowed to be offered at reserve, at node $n$ .
$W_n$	The maximum total amount of generation and reserve, offered by the generator, at node $n$ .
$\mathcal{N}$	The set of all nodes in the network. Note that in our model we have one agent per node. This is not a restrictive assumption.
$\mathcal{A}$	The set of all arcs in the network.
$\mathcal{N}_e$	The set of all nodes in zone $e$ .
$L$	The loop constraint matrix, where $L_{l,ij}$ corresponds to row $l$ (associated with each loop) and the column $ij$ corresponds to arc $ij$ .

$\mathcal{T}_c^n$	The set of interruptible consumption tranches.
$e_n$	indicates the zone that node $n$ is located in.
$\mathcal{E}$	The set of zones.
$\mathcal{Z}$	The set for types of tranches, i.e. consumption, generation, ILR and reserve. $\mathcal{Z} = \{c, g, rc, rg\}$
$\mathcal{T}_z$	The set of all offered tranches of type $z$ .
$\mathcal{T}_z^n$	The set of all tranches of type $z$ at node $n$
$x_t^z$	The variable associated with the dispatch quantity tranche type $z$ .
$p_t^z$	The price of tranche $t$ of type $z$ .
$q_t^z$	The quantity of tranche $t$ of type $z$ .
[ ]	Variables in [ ] indicate the duals of their associate constraints.

$$[\text{D-LP}] \max_{x^c, x^g} \sum_{t_c \in \mathcal{T}_c} p_{t_c}^c x_{t_c}^c - \sum_{t_g \in \mathcal{T}_g} p_{t_g}^g x_{t_g}^g - \sum_{t_{rg} \in \mathcal{T}_{rg}} p_{t_{rg}}^{rg} x_{t_{rg}}^{rg} - \sum_{t_{rc} \in \mathcal{T}_{rc}} p_{t_{rc}}^{rc} x_{t_{rc}}^{rc}$$

$$\text{s.t.} \quad \sum_{t_c \in \mathcal{T}_c^n} x_{t_c}^c + \sum_{i|ni \in \mathcal{A}} f_{ni} - \sum_{i|in \in \mathcal{A}} f_{in} = \sum_{t_g \in \mathcal{T}_g^n} x_{t_g}^g \quad [\pi_n^d] \quad (2.1)$$

$$- \sum_{n \in \mathcal{N}_e} \sum_{z \in \{rc, rg\}} \sum_{t_z \in \mathcal{T}_z^n} x_{t_z}^z = -r_e \quad [\pi_{e_n}^r] \quad (2.2)$$

$$\sum_{ij \in \mathcal{A}} L_{i,j} f_{ij} = 0 \quad [\lambda_l] \quad (2.3)$$

$$-K_{ij} \leq f_{ij} \leq K_{ij} \quad [\eta_{ij}^+, \eta_{ij}^-] \quad (2.4)$$

$$0 \leq x_{t_z}^z \leq q_{t_z}^z \quad [\nu_{t_z}^{z+}, \nu_{t_z}^{z-}] \quad (2.5)$$

$$\sum_{t_{rc} \in \mathcal{T}_{rc}^n} x_{t_{rc}}^{rc} - \sum_{t_c \in \mathcal{T}_c^n} x_{t_c}^c \leq 0 \quad [\theta_n] \quad (2.6)$$

$$\sum_{t_{rg} \in \mathcal{T}_{rg}^n} x_{t_{rg}}^{rg} \leq B_n \sum_{t_g \in \mathcal{T}_g^n} x_{t_g}^g \quad [\phi_n] \quad (2.7)$$

$$\sum_{t_{rg} \in \mathcal{T}_{rg}^n} x_{t_{rg}}^{rg} + \sum_{t_g \in \mathcal{T}_g^n} x_{t_g}^g \leq W_n \quad [\phi'_n]. \quad (2.8)$$

Here (2.1), and (2.6) to (2.8) hold  $\forall n \in \mathcal{N}$ . (2.2) holds  $\forall e \in \mathcal{E}$ . (2.3) holds for each loop, indicating that sum of impedance adjusted flows across the loop must be zero. (2.4) holds  $\forall ij \in \mathcal{A}$ . (2.5) holds  $\forall t_z \in \mathcal{T}_z, \forall z \in \mathcal{Z}$ .

In order to capture the co-optimized strategic behaviour, we lay out a bi-level optimization problem, which has the OPF problem as the lower level problem. We start with the deterministic model, in which we assume that the strategic consumer maximizes its utility by consuming its optimal demand level  $y_n^d$  (with the capacity of consumption  $C_n^d$ ), and offering optimal ILR level  $y_n^r$  (with the capacity of ILR  $C_n^r$ ), while taking into account the amount of un-interruptible load ( $V_n$ ). Note that in order to determine the strategic node, we set the  $C_n^d$  and  $C_n^r$  to positive values for the strategic node  $n$ , and at the rest of nodes  $C_n^d$  and  $C_n^r$  are set to be zero.

In section 4, we will extend this model for a stochastic setting, in which the consumer submits optimal bid and offer *curves* instead of optimal quantities of energy and ILR. Here, the electricity market clearing problem [D-LP] is embedded within the price-making consumer's profit optimization problem, rendering a leader-follower type model captured as a bi-level program.

In addition, we denote the utility function for consuming electricity (for the strategic consumer) as  $\mathcal{U}(y_n^d)$ . Without loss of generality, we use a constant marginal utility of consumption ( $u$ ), which yields  $\mathcal{U}(y_n^d) = uy_n^d$ , however, any concave utility function is applicable to our model. The objective of our problem is to maximize the profit of the major consumer, which consists of the utility of consuming electricity and revenues obtained through ILR, minus the cost of consumption. Moreover, the cost of offering ILR can be embedded within the utility function; such cost only occurs in the case that the major consumer is actually called upon to interrupt its load. We define the probability of being called upon as  $\rho^r$ . Hence, the objective function will be:  $\sum_{n \in \mathcal{N}} (u - \pi_n^d)(y_n^d - \rho^r y_n^r) + \pi_{e_n}^r y_n^r$ , where in practice  $\rho^r \simeq 0$ . Therefore, for the sake of simplicity

(and generally without any effect on the optimal solution<sup>1</sup>), we set  $\rho^r = 0$  in the objective function of our model in this section. We lay out the bi-level optimization problem for our single node example that we call [B-L], as below:

$$\begin{aligned} \text{[B-L]} \quad & \max_{y_n^d, y_n^r} \sum_{n \in \mathcal{N}} \left( u y_n^d - \pi_n^d y_n^d + \pi_{e_n}^r y_n^r \right) \\ \text{s.t.} \quad & 0 \leq y_n^d \leq C_n^d \end{aligned} \quad (2.9)$$

$$0 \leq y_n^r \leq C_n^r \quad (2.10)$$

$$y_n^d - y_n^r \geq V_n \quad (2.11)$$

$$\text{[D-LP2]} \quad \max_{x^z | z \in \mathcal{Z}} \sum_{t_c \in \mathcal{T}_c} p_{t_c}^c x_{t_c}^c - \sum_{t_g \in \mathcal{T}_g} p_{t_g}^g x_{t_g}^g - \sum_{t_{rg} \in \mathcal{T}_{rg}} p_{t_{rg}}^{rg} x_{t_{rg}}^{rg} - \sum_{t_{rc} \in \mathcal{T}_{rc}} p_{t_{rc}}^{rc} x_{t_{rc}}^{rc}$$

$$\text{s.t.} \quad (2.3) - (2.8)$$

$$\sum_{t_c \in \mathcal{T}_c^n} x_{t_c}^c + \sum_{i | ni \in \mathcal{A}} f_{ni} - \sum_{i | in \in \mathcal{A}} f_{in} = \sum_{t_g \in \mathcal{T}_g^n} x_{t_g}^g - y_n^d \quad [\pi_n^d] \quad (2.12)$$

$$- \sum_{n \in \mathcal{N}_e} \sum_{z \in \{rc, rg\}} \sum_{t_z \in \mathcal{T}_z^n} x_{t_z}^z = \sum_{n \in \mathcal{N}_e} y_n^r - r_e \quad [\pi_e^r]. \quad (2.13)$$

Here (2.9) to (2.12) hold  $\forall n \in \mathcal{N}$ , whereas (2.13) holds  $\forall e \in \mathcal{E}$  (reserve needs are measured and met on the zonal level). We call the market clearing problem in the bi-level model [D-LP2]. The difference between this OPF problem and the previous version ([D-LP]) is adding the upper level variables  $y_n^d$  and  $y_n^r$  in (2.12) and (2.13) as fixed demand and ILR for the lower level problem; this is equivalent to bidding energy at infinite price and offering ILR at zero price, to insure full dispatch. These two sets of variables are deemed to be constants in the primary dispatch model [D-LP2]. Note that, our bi-level optimization model allows for the strategic consumer to be located at several grid exit points. However, for the purpose of this paper (NZAS), the strategic consumer is located at one node in the network. Therefore, without loss of generality we use  $y^d$  and  $y^r$  to denote the strategic node's energy consumption and ILR level, and use  $\pi^d$  and  $\pi^r$  to denote the corresponding energy and reserve price at the strategic node.

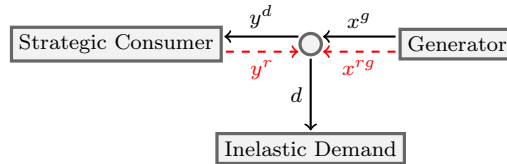


Fig. 1: The single-node network.

We proceed with a simple example based at a single node, depicted above. We demonstrate that co-optimized reserve offering makes a significant difference to the optimal consumption strategy and ought not be left out of the decision making process. In this example we have 3 agents: a generator who submits an energy offer stack and a reserve offer stack; a consumer with inelastic demand ( $d$ ); and a major consumer capable of demand response and offering ILR, as depicted in Fig. 1. Table 1 demonstrates the parameter values that we use in this example, as well as Table 2, in which the generation and reserve offer stacks of the generator are shown. Note that given this example is based on a single-node, for the sake of simplicity, we omit the node ( $n$ ) subscripts from parameters and variables notation.

<sup>1</sup> In NZEM, the average number of times reserve is triggered is 2 times over a year [24]. Given the number of trading periods in a year ( $48 \times 365 = 17520$ ) the  $\rho^r$  value in our case study is approximately 0.0001%.

Parameter	$u$	$W$	$B$	$V$	$r$	$C^d$	$C^r$	$\mathcal{T}_g$	$\mathcal{T}_{rg}$	$d$
Value	190	255	1	0	97	100	100	{1,2,...,8}	{1,2,...,8}	65-130

Table 1: Parameter Values of the Single Node Example

Tranche	Energy Stack		Reserve Stack		
	$t$	$p_t^g$	$q_t^g$	$p_t^{rg}$	$q_t^{rg}$
1		17	25	13	15
2		29	15	39	30
3		51	18	57	28
4		76	16	67	25
5		90	22	98	24
6		119	20	110	12
7		126	25	129	22
8		200	90	200	100

Table 2: Energy and reserve offer stack data for the generator.

Below we report on the optimal consumption and ILR values for the major consumer who solves [B-L], for different levels of  $d$ . In order to show the impact of strategic co-optimization of electricity and reserve, we construct two versions of this example. First we assume that the major consumer is only allowed to submit its consumption quantity, but does not offer ILR (by adding the constraint  $y^r = 0$  to [B-L]); we call this V1. For comparison, in model V2, the major consumer is able to offer any fixed quantity of ILR up to the level of consumption, (i.e.  $0 \leq y^r \leq y^d$ ), while simultaneously determining the optimal consumption quantity. To present a comprehensive illustration of the optimal behavior of the major consumer, we run a sensitivity analysis by changing the quantity of inelastic demand; this entails solving V1 and V2 for varying levels of  $d$  (from 65 to 130 with an increment of one), and plotting the rendered optimal values.

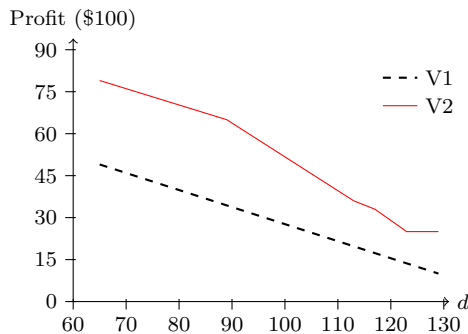


Fig. 2: Profit maximizing objective function

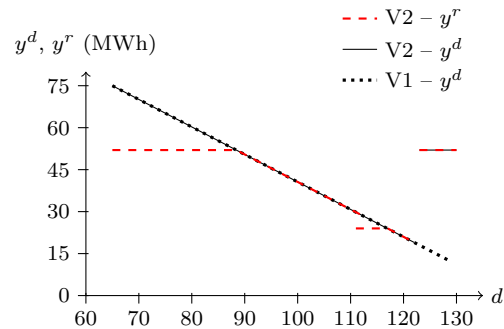


Fig. 3: Strategic consumer decision variables

Fig. 2 demonstrates the optimal utility of the large consumer from V1 and V2 experiments. It shows that the consumer's optimal profit decrease as the in-elastic demand increases. Also, as anticipated, the results of this experiment show more profit in the co-optimized energy and reserve version, V2.

Next, we report on the optimal values of  $y^d$  and  $y^r$  for the two experiments. Note that, as shown in Fig. 3, in V2, the optimal ILR offer (dotted curve) is never above the electricity consumption, demonstrating the requirement that the consumer can not offer any more ILR ( $y^r$ ) than the quantity it consumes ( $y^d$ ). The flat areas of ILR offer curve show that, initially the consumer withholds from offering the maximum available amount of ILR ( $y^d = y^r$ ) to utilize getting paid higher prices of reserve for its ILR offer. This pattern persists up to  $d = 122$ , where we observe a sudden increase in both electricity consumption and ILR offer. Although more consumption results in higher electricity prices, this cost is offset by being able to offer more ILR. On the other hand, in the absence of the option to supply ILR (i.e. V1), optimal consumption  $y^d$  decreases as a function of the inelastic demand, in such a way that the total demand (that of the major consumer plus the inelastic demand) remains constant. This illustrates the significant difference in the consumption strategy, depending on the ability to offer ILR.

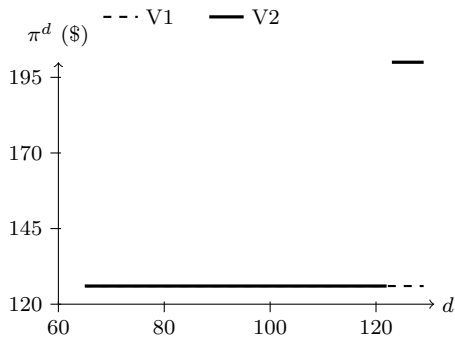


Fig. 4: Electricity prices

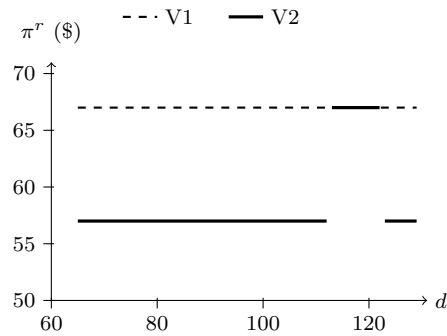


Fig. 5: Reserve prices

The last set of results pertains to the clearing prices for energy  $\pi^d$  for the experiments (illustrated in Fig. 4) and reserve prices  $\pi^r$  (illustrated in Fig. 5). We observe a jump in electricity price in V2, which is a result of a sudden increase in electricity consumption<sup>2</sup>. For the major consumer, this rise in electricity cost is compensated for by being paid more for ILR. On the other hand, the electricity price remains constant in experiment V1. Here, the major consumer is able to keep the price at \$126, by decreasing its own demand to cancel out the increase in the inelastic demand (as already observed in Fig. 3).

Reserve price is also affected by ILR offers of the strategic consumer. In V2, for each level of inelastic demand, the reserve price is at most equal to that of the V1. Note that in V2, with the participation of the major consumer in the reserve market, the resulting reserve prices become lower. The above results show that major consumers who strategically co-optimize their energy bids and reserve offers are able to improve their return.

## 2.2 Contrast to previous attempts

Strategic bidding problems that are addressed in several papers (see e.g., [17, 18, 20]) look similar to our model at first glance. However [17, 18] essentially ignore the reserve complexity, by assuming that the consumer is a price taker in that aspect. Furthermore, the standard MPEC (Mathematical Program with Equilibrium Constraints) to MIP reformulations used in [17, 18] are unable to handle our large-scale and more complex problems. In [20, 21], Cleland et al. introduce a stochastic simulation based model (BOOMER-consumer) to solve the co-optimization of demand and reserve over a realistic network platform. They solve the problem of what *fixed* optimal quantity to consume and what optimal reserve stack (coupled with this consumption quantity) to offer. In contrast, we address the real problem of offering the optimal *demand bid curve* and reserve offer to the market. To clarify these differences, we present an example (based on a large consumer in the South Island of NZ), and compare our model to the BOOMER-consumer method. Our sample space consists of 6 different scenarios from historical data of winter 2017 (publicly available at [25]). The aim is to produce optimal (in expectation) reserve stacks, while taking into account the co-optimization of reserve and energy in the NZEM. In order to make the optimal reserve stack, BOOMER fixes the consumption level and calculates the optimal reserve stack (in expectation) for a given consumption level. (For the sake of simplicity, we limit our example to only 3 consumption levels.) Following the BOOMER method ([20, 21]), we construct these optimal reserve stacks. Table 3 presents the details of optimal solution values of reserve stacks for each consumption level, and Figure 6 plots these reserve stacks.

For comparison, we solve the same problem using our stochastic bi-level optimization model (See section 4 for the detailed description of this stochastic optimization problem). The output

<sup>2</sup> Note that in this example we observe that only with  $d \geq 126$ , the energy price becomes higher than  $u$ . But although  $u = 190$ , and the price of energy is \$197, since the price of reserve is \$57, it is still in the interests of the consumer to consume. However, if the marginal utility of consuming electricity for the strategic consumer was not high enough, the optimal action would be to consume much less energy, or none at all to avoid a negative profit.



Table 3: BOOMER optimal reserve stack details

Consumption	400		600		700	
Scenario	$y^r$	$\pi^r$	$y^r$	$\pi^r$	$y^r$	$\pi^r$
a	0	0	0	0	0	0
b	2.362	0.5	5.049	0.5	37.997	0.5
c	2.362	6	5.049	6	67.652	0.5
d	22.643	43	28.642	74.1	67.652	15
e	2.362	42.1	24.365	15	67.652	0.5
f	2.362	15	5.049	15	67.652	0.5

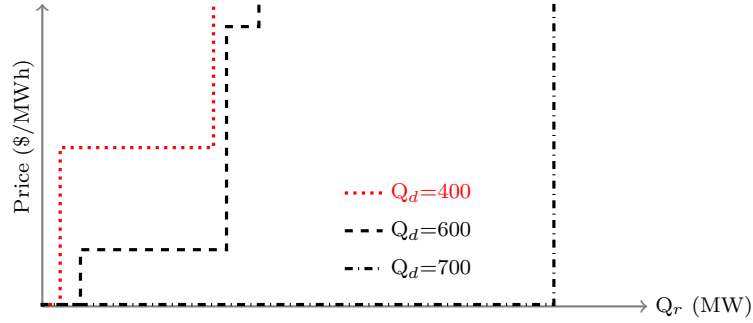


Fig. 6: BOOMER optimal wait-and-see reserve offers.

of our model will be two stacks that maximize the expected profit. Table 4 presents the optimal solution values obtained from the bi-level method. Also, the corresponding monotone stacks are shown in Figures 7 and 8.

Table 4: co-optimized optimal stacks

Scenario	$y^d$	$\pi^d$	$y^r$	$\pi^r$
a	292.875	55	2.362	0
b	379.316	55	2.362	0.5
c	396.97	55	2.362	6
d	506.459	55	22.643	44
e	489.268	55	2.362	43.1
f	540.662	55	2.362	15

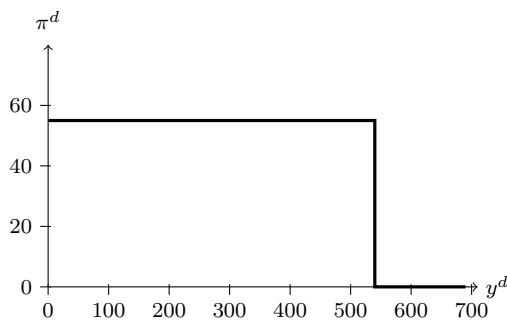


Fig. 7: Co-optimized demand bid

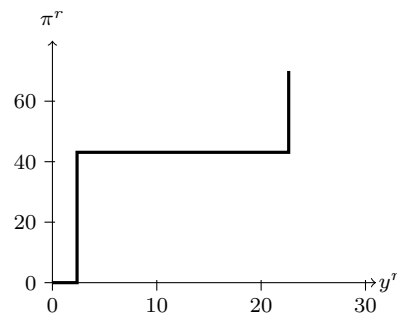


Fig. 8: Co-optimized reserve offer

The reserve stacks in the BOOMER-consumer method are better informed as they are tailored for a particular consumption level. However, the reserve offer that is derived from our model is optimized in expectation for various levels of consumption, which means it provides a here-and-now

action rather than a wait-and-see approach. In order to complete this comparison, we report on the difference in profit between the two methods in Table 5. Here, the bi-level method shows a better performance on average, in comparison with each of the designated consumption levels.

Table 5: Expected profit comparison

Method	BOOMER			Bi-level
Consumption	400	600	700	
Expected Profit	12931.98	3826.73	-11493.8	15390.52

Note that while it is possible to optimize for the 'best' fixed quantity, the BOOMER-consumer method simply does not provide the flexibility for the consumer to respond in real-time to market volatility. In what follows we will present our approach for constructing optimal bid and offer curves over complex networks, with many scenarios.

### 3 Bi-level to MIP reformulation methods

A common approach to solve a bi-level problem is through reformulating it as an MPEC by replacing the lower-level problem with its optimality conditions. However, most standard MPEC solvers will not guarantee global optimality due to non-convexities arising from the optimality conditions of the lower level problem. Therefore, to find a global optimum, we reformulate [B-L] as a MIP. Following [26] and [27] we use the KKT conditions of the dispatch problem, and binary variables with big-M right-hand sides to enforce the complementary constraints. This technique is used in [28] and [29] to convert a profit maximizing bi-level optimization problem to a MIP (to optimize generator offer strategies). In [30], binary expansion is used to reformulate the day-ahead market MPEC problem to a MIP, but their approach did not scale for the examples over a network with several generators. In addition to the complexity of solving the MIP over a large network, our model must also capture the co-optimization of energy and reserve (note that reserve and electricity prices are linked by the constraints (2.7) and (2.8)). Although, in theory, this reformulation will enable us to find the global optimum, the nature of integer optimization impedes efficient solution times; in fact, the problems become can intractable with the introduction of uncertainty. In subsection 3.1 we introduce a novel reformulation method and further compare it with the performance of the standard MIP reformulations in section 5.

#### 3.1 Bi-parametric sensitivity analysis reformulation method

Here we present a reformulation method to solve [B-L] using a novel bi-parametric sensitivity analysis algorithm. The idea is to explicitly capture reserve and energy prices at a node  $n$ , as functions of the actions of the strategic consumer who is located at that node, using the fundamentals of the simplex method<sup>3</sup>. In practice, the bi-level problem is solved over a complex electricity market, that operates over a large network. For instance, there are approximately 500 nodes (grid exit and injection points) in the NZEM, however the only nodal prices that affect our decisions are those corresponding to the strategic consumer's node. If we can find the energy and reserve prices as functions of the consumer's actions, i.e  $(\pi_d, \pi_r) = f(y^d, y^r)$ , each scenario could be reduced to a point-to-set mapping for prices, instead of modelling all the details of the dispatch problem that results in a large and complex MIP.

Here we use sensitivity analysis on the right-hand sides of the two constraints that determine the nodal energy and reserve prices in the lower level problem for the major consumer. In [B-L], these two constraints are (2.12) and (2.13). By employing an iterative algorithm, we define regions

<sup>3</sup> This method, when applied to a multi-node network, permits the strategic consumer to be located at a single node. Our algorithm is not immediately applicable for a strategic consumer who purchases electricity at multiple nodes (i.e. the consumer that owns plants located at different nodes in the market).

corresponding to optimal bases of the lower-level optimization problem [D-LP2]. For each basis, there exists a pair of prices  $(\pi^d, \pi^r)$  which are constant with respect to the right-hand side terms  $(y^d, y^r)$  while that basis is optimal. In Appendix A, we lay out a detailed algorithm for reducing a generic LP into a point-to-set mapping using our bi-parametric sensitivity analysis method.

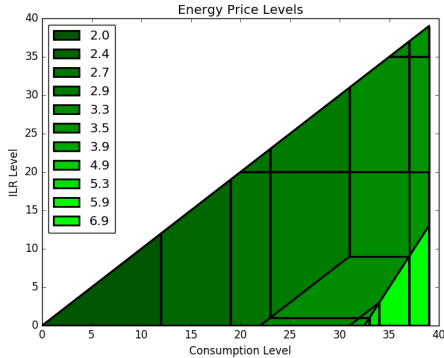


Fig. 9: Energy Price Regions

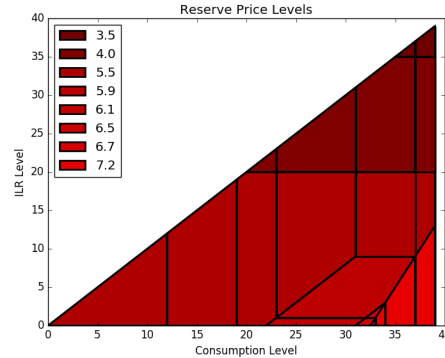


Fig. 10: Reserve Price Regions

Figures 9 and 10 demonstrate the decomposed regions, defined by the vertices obtained through our bi-parametric sensitivity analysis, for an example over a 4-node network. Here regions are shown from a top-down perspective. These regions are divided by black lines, where each depicted region has corresponding constant reserve and energy prices. In order to address the possible degeneracy of solutions<sup>4</sup>, we have assigned “vertical regions” to the edges of the depicted regions (for further detail on this see appendix A).

In Fig. 9 each shade corresponds to a set of actions by the consumer over which the price of energy is constant. Similarly, Fig. 10 presents the set of actions over which the price of reserve is constant (depicted by shades of red). Note that the regions are identical in both figures. Also note that the price of energy and reserve increase as the level of consumption increases, and the energy and reserve prices decrease as the consumer offers more ILR.

This reformulation method simplifies the lower level problem, while keeping the exact information regarding the interactions of strategic consumer’s consumption and ILR with the market. For instance, Figures 9 and 10 can show the effect of offering ILR, when the other generators in the market are at their maximum capacity; where regions with tilted lines represent a state of the market in which a generator has a binding inverse bathtub constraint.

#### 4 Stochastic demand response

In section 3, we assumed full information about the electricity market, including information on bids and offers of other market participants. While a deterministic model is a useful starting point, in reality we are exposed to uncertainty and lack of information on the market data. To address this, we develop a stochastic version of our model, where the consumer faces a set of scenarios  $\Omega$  with probability  $\rho_\omega$  for scenario  $\omega \in \Omega$ . These scenarios can capture different sources of uncertainty, including, but not limited to, different levels of system demand, and different generation offers. Therefore, in order to find the optimal consumption  $(y^{d^\omega})$  and ILR  $(y^{r^\omega})$  for each scenario  $\omega$ , we lay out a stochastic optimization problem by solving the standard [MIP] model (described in section 3), for each scenario over the set  $\Omega$ , and obtain the optimal expected profit. We call this problem [S-MIP].

In order to reduce complexity of this stochastic model, we employ the bi-parametric sensitivity analysis reformulation and compute (pre-determine) the regions corresponding to the full NZEM dispatch problem, for each scenario. Subsequently, we lay out a mixed integer program (presented

<sup>4</sup> Degenerate solutions may occur at the edge of regions, where the price of energy or reserve could be a convex combination of prices of the two adjacent regions.

as  $[\alpha\text{-MIP}]$ ) that reads in the regions corresponding to each scenario  $\omega$  ( $\forall \omega \in \Omega$ ) and outputs the optimal expected reserve and energy stacks over  $\Omega$ , that yield the maximum expected profit for the major consumer.

Assume that  $R^\omega$  is the set of all regions retrieved from the algorithm described in section 3.1, for scenario  $\omega$ , and  $R_i^\omega$  as the set of all the extreme points that form region  $i$  in  $R^\omega$ . In this model, each extreme point  $j$ , within region  $i$ , in set  $\mathcal{R}^\omega$ , is defined by the following four parameters: the corresponding consumption level, reserve level, energy and reserve prices, that are denoted by  $\hat{y}_{i,j}^\omega$ ,  $\hat{y}_{i,j}^{r\omega}$ ,  $\hat{\pi}_{i,j}^{d\omega}$  and  $\hat{\pi}_{i,j}^{r\omega}$ , respectively.

In  $[\alpha\text{-MIP}]$ ,  $y^{d\omega}$ ,  $y^{r\omega}$ ,  $\pi^{d\omega}$  and  $\pi^{r\omega}$  are the variables corresponding to strategic consumption, ILR, and strategic node's energy and reserve price, respectively, for each scenario  $\omega$ . Also, we define  $\psi^{d\omega}$  and  $\psi^{r\omega}$  as the variables corresponding to cost of consumption ( $y^{d\omega} \pi^{d\omega}$ ) and revenue of ILR ( $y^{r\omega} \pi^{r\omega}$ ) in scenario  $\omega$ , respectively. In this formulation we use binary variable  $z_i^\omega$  to determine which region to choose in scenario  $\omega$ . We called this mathematical program  $[\alpha\text{-MIP}]$  due to the use of  $\alpha$  variables that define the convex hull representing each region.

$$\begin{aligned}
[\alpha\text{-MIP}] \quad & \max_{y^d, y^r, z} \sum_{\omega \in \Omega} \left( u \times y^{d\omega} - \psi^{d\omega} + \psi^{r\omega} \right) \\
\text{s.t.} \quad & \psi^{d\omega} = \sum_{i \in \mathcal{R}^\omega} \sum_{j \in \mathcal{R}_i^\omega} \alpha_{i,j}^\omega \hat{y}_{i,j}^{d\omega} \hat{\pi}_{i,j}^{d\omega} & \forall \omega \in \Omega \\
& \psi^{r\omega} = \sum_{i \in \mathcal{R}^\omega} \sum_{j \in \mathcal{R}_i^\omega} \alpha_{i,j}^\omega \hat{y}_{i,j}^{r\omega} \hat{\pi}_{i,j}^{r\omega} & \forall \omega \in \Omega \\
& y^{d\omega} = \sum_{i \in \mathcal{R}^\omega} \sum_{j \in \mathcal{R}_i^\omega} \alpha_{i,j}^\omega \hat{y}_{i,j}^{d\omega} & \forall \omega \in \Omega \\
& y^{r\omega} = \sum_{i \in \mathcal{R}^\omega} \sum_{j \in \mathcal{R}_i^\omega} \alpha_{i,j}^\omega \hat{y}_{i,j}^{r\omega} & \forall \omega \in \Omega \\
& \pi^{d\omega} = \sum_{i \in \mathcal{R}^\omega} \sum_{j \in \mathcal{R}_i^\omega} \alpha_{i,j}^\omega \hat{\pi}_{i,j}^{d\omega} & \forall \omega \in \Omega \\
& \pi^{r\omega} = \sum_{i \in \mathcal{R}^\omega} \sum_{j \in \mathcal{R}_i^\omega} \alpha_{i,j}^\omega \hat{\pi}_{i,j}^{r\omega} & \forall \omega \in \Omega \\
& \sum_{j \in \mathcal{R}_i^\omega} \alpha_{i,j}^\omega = z_i^\omega & \forall i \in \mathcal{R}^\omega, \forall \omega \in \Omega \\
& \sum_{i \in \mathcal{R}^\omega} z_i^\omega = 1 & \forall \omega \in \Omega \\
& 0 \leq \alpha_{i,j}^\omega \leq 1 & \forall j \in \mathcal{R}_i^\omega, \forall i \in \mathcal{R}^\omega, \forall \omega \in \Omega \\
& z_i^\omega \in \{0, 1\} & \forall i \in \mathcal{R}^\omega, \forall \omega \in \Omega
\end{aligned}$$

When we solve  $[\alpha\text{-MIP}]$ , optimal values of  $y^{d\omega}$ ,  $y^{r\omega}$ ,  $\pi^{d\omega}$  and  $\pi^{r\omega}$  would form the optimal points corresponding to scenario  $\omega$ . However, our aim is to calculate two admissible optimal stacks (the consumer's demand-side bid and ILR offer), that are optimal in expectation over all scenarios. In order for the optimal stacks to be admissible to the market, they must be monotone step functions. In particular, the bid stack must be decreasing and the ILR stack increasing. In subsection 4.1 we discuss the implementation of monotonicity constraints and its impact on solution time.

#### 4.1 Monotone bids

In the single-scenario case, and in the absence of reserve and over a single-node market, the optimal consumption level is effectively singled out by the quantity that determines the dispatch on the (aggregate market) residual supply function. The seminal paper of Klemperer and Meyer [31] lays out the premise for using supply functions as such offers adapt better to uncertain environments faced with multiple scenarios.

It is tempting to determine the optimal quantity of consumption for each scenario, in isolation. The problem with this approach is that the sequence of these consumption decisions may not support a monotone curve. Fig. 11 demonstrates the optimal points obtained by solving [B-L] without applying any monotonicity constraints for four sample scenarios (1 – 4). Here we demonstrate each scenario's residual supply stack (with lines), and the corresponding (anticipating) optimal consumption value (with points). Note that there is no single monotone decreasing demand curve that can pass through these 4 points.

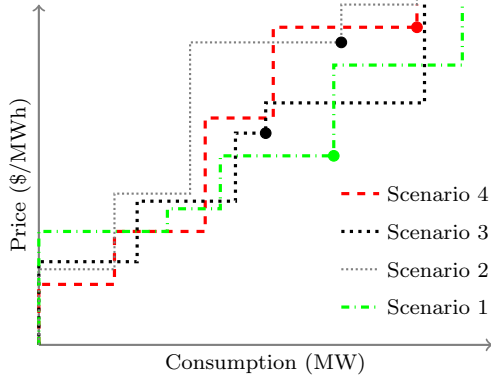


Fig. 11: Optimal wait-and-see bids.

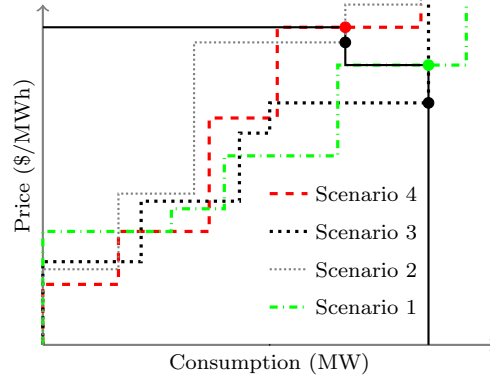


Fig. 12: Optimal monotone consumer bid.

To construct admissible bids and offers, we add monotonicity constraints on the resulting bid and offer curves. We define binary variables  $\zeta_{ij}^d$  to construct a monotone decreasing energy bid stack, where we ensure that the energy price in scenario  $i$  is higher than that of  $j$ , provided the quantity consumed in scenario  $i$  is less than scenario  $j$ . Similarly for the ILR offer, we define variables  $\zeta_{ij}^r$  that ensure monotonicity of the ILR stack, however for the ILR offer, we ensure that the stack is monotonically increasing. Once the problem is solved with the monotonicity constraints included, we obtain a monotone solution as depicted in Fig. 12.

$$y^{d^i} \leq y^{d^j} + M^d \zeta_{i,j}^d \quad \forall i, j \in \Omega, i \neq j \quad (4.1)$$

$$y^{r^i} \leq y^{r^j} + M^r \zeta_{i,j}^r \quad \forall i, j \in \Omega, i \neq j \quad (4.2)$$

$$\pi^{d^i} \geq \pi^{d^j} - M^\pi \zeta_{i,j}^d \quad \forall i, j \in \Omega, i \neq j \quad (4.3)$$

$$\pi^{r^i} \leq \pi^{r^j} + M^\pi \zeta_{i,j}^r \quad \forall i, j \in \Omega, i \neq j \quad (4.4)$$

$$\zeta_{i,j}^d + \zeta_{j,i}^d = 1 \quad \forall i, j \in \Omega, i \neq j \quad (4.5)$$

$$\zeta_{i,j}^r + \zeta_{j,i}^r = 1 \quad \forall i, j \in \Omega, i \neq j \quad (4.6)$$

$$\zeta_{i,j}^d, \zeta_{i,j}^r \in \{0, 1\} \quad \forall i, j \in \Omega, i \neq j \quad (4.7)$$

In order to implement the monotonicity constraints within our stochastic models, we add constraints (4.1)–(4.7) to [S-MIP] and [ $\alpha$ -MIP]. When solving these models with multiple scenarios, the number of constraints and variables increase proportionally with the square of the number of scenarios. In addition, the monotonicity constraints link the scenarios together, meaning that decisions in one scenario may affect the other scenarios' optimal solutions. This yields a large MIP, which can become computationally intractable with a large number of scenarios. Section 5 contains numerical results of implementing our algorithm, and a comparison of the performances of [S-MIP] and [ $\alpha$ -MIP].

## 5 Numerical results

In this section we focus on implementing our optimization policies for a major consumer of electricity in New Zealand. The strategic consumer in our case study is the New Zealand Aluminium

Smelter (NZAS), which is located in the South Island of New Zealand. Given that the NZAS’s consumption is roughly 15% of the whole New Zealand demand, we assume that this major consumer is a price-maker agent which submits bid and offers to the NZEM’s co-optimized OPF every half-hour. Therefore, using the reformulation [ $\alpha$ -MIP] from section 4, we solve the bi-level optimization problem from section 2, which maximizes the profit for the major consumer. However, in this case we embed the full-scale NZEM’s OPF (as the lower-level problem). Furthermore, to address uncertainty, we introduce multiple scenarios and optimize the expected profit over a sample set as was discussed in section 4.1. In order to construct the sample set of scenarios, we use historical data which is publicly available online at the New Zealand Electricity Authority’s EMI repository [25].

First, we briefly compare the size and solution time of the two proposed reformulated stochastic co-optimization models, [S-MIP] and [ $\alpha$ -MIP], when implemented for the NZAS. Table 6 presents the average optimality gap for [S-MIP] and [ $\alpha$ -MIP], after one hour of solution time (the symbol - in this table indicates that no gap is available as no incumbent was found in the time-frame). Similarly, Table 7 compares the number of integer variables in each method, given the sample size. The [S-MIP] model can only solve models with up to ten scenarios, in a reasonable time frame. On the other hand, [ $\alpha$ -MIP] solves the same ten-scenario models in (on-average) 3 minutes. Given the [ $\alpha$ -MIP] method’s computational advantage in allowing us to incorporate larger number of scenarios in the model, we use the [ $\alpha$ -MIP] optimization problem for our full-scale NZAS case-study.

Table 6: Average bound gaps (%) versus number of scenarios.

Method	Number of scenarios									
	4	6	8	10	12	14	16	18	20	22
S-MIP	0	12.01	33.61	86.32	-	-	-	-	-	-
$\alpha$ -MIP	0	0	0	0	0	0	0	0	0.8	4.9

Table 7: Number of integers versus number of scenarios.

Method	Number of scenarios									
	4	6	8	10	12	14	16	18	20	22
S-MIP	10504	16961	21078	26388	31710	37048	42350	47648	52988	58360
$\alpha$ -MIP	1101	1838	2392	3342	3744	3991	4677	5237	5924	6332

In order to compute the optimal policies (stacks), we need to choose a sample of scenarios ( $\Omega$ ) from the scenario space. Submitting optimal (in expectation) bid and offer stacks is a here-and-now action which accounts for different types of time-periods, therefore finding the right combination of scenarios significantly improves the performance of such decisions. If we build our scenario set from many similar time-periods that are more likely to happen in the future, we miss the outlier scenarios which could possibly be incorporated in the bid stack, without altering the optimal response to the more frequent scenarios. Hence, we avoid picking very similar scenarios in our scenario set (e.g. two consecutive time-periods in one day), and instead use a representative scenario. This, not only enhances the solution time, by reducing the symmetry in the MIP (and the resulting fractionality), but also enables the major consumer to optimize for various types of time periods, through incorporating more tranches in the optimal stacks. In appendix B, we provide two examples that develop intuition on the importance of diverse scenario sampling.

In what follows, we simulate our proposed algorithm for the winter peak time-periods. At each iteration of our simulation, in order to define the set  $\Omega$ , we randomly choose 20 scenarios, from a scenario space consisting of 200 trading-periods from morning peaks, in July and August 2016 and 2017. We construct random sets of  $\Omega$ , that represent different types of time periods. Note that 2016 and 2017 were relatively different years in terms of energy prices, and when combined would represent a wide range of scenarios. Hence, we have assigned scenarios to 4 different clusters,

based on the average South Island energy prices in the morning-peak trading periods (6am–10am). The sampling scheme is to pick scenarios from all the clusters, in order to capture the diversity of scenarios.

After sampling a scenario set, we compute the optimal dispatchable demand and ILR stacks by solving  $[\alpha\text{-MIP}]$ . Figure 13 shows the optimal bid stacks for the NZAS for one of the sampled scenario sets, when calculated for different marginal values of electricity consumption ( $u$ ).

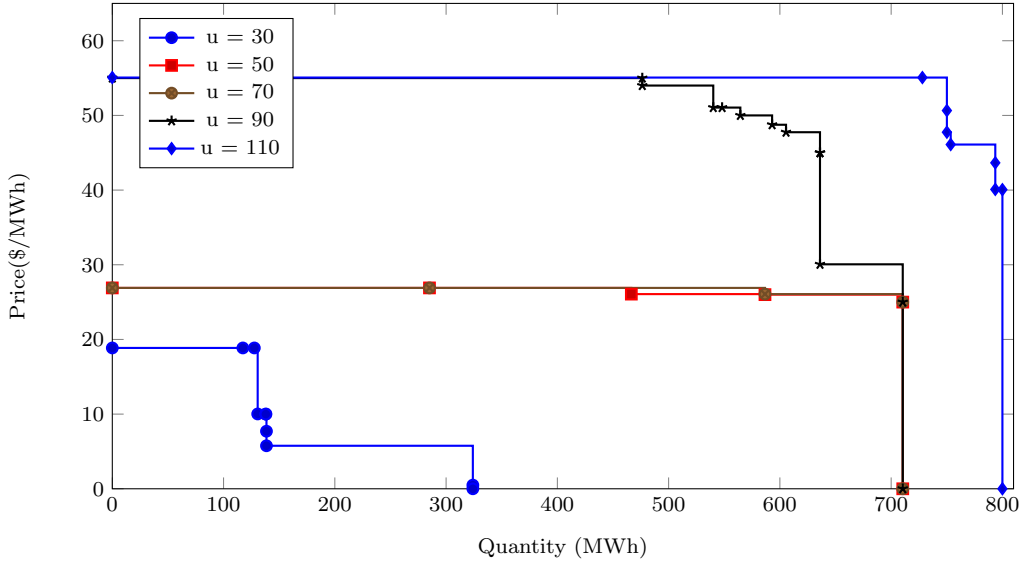


Fig. 13: Optimal energy bid stack - winter peak

Subsequently, these optimal stacks need to be submitted to the co-optimized OPF, which renders the dispatched quantities and prices for the upcoming realized scenario. Therefore, in the following experiment we test the performance of the optimal stacks that are derived from historical data through simulating them (i.e. submitting the stacks to the co-optimized OPF) for 100 out-of-sample scenarios, and report on the average expected gained profit. Figure 14 presents the stages of the algorithm in an illustrative diagram.

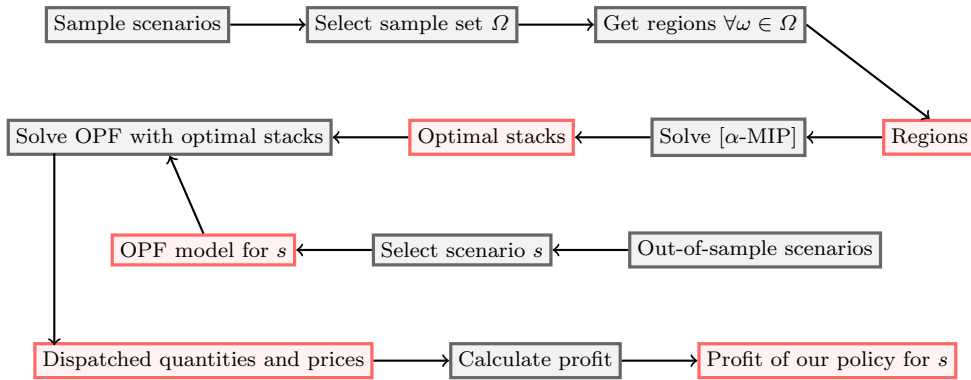


Fig. 14: Optimal stack policy out-of-sample simulation algorithm.

Finally, we compare our proposed policy with the clairvoyant optimization<sup>5</sup> (which is an absolute upper bound on profit) and the fixed quantity that is consumed by NZAS in practice. Table 8 outlines the average results of 200 simulations. The experiment is done over different levels of

<sup>5</sup> The clairvoyant policy is calculated by solving the deterministic MIP model with the realized scenario's parameter values.

electricity consumption's marginal value ( $u$ ) to compare the performance of our proposed policy over a broader range of parameters<sup>6</sup>. The first column of this table shows the different marginal value levels. The second column demonstrates the average profit over out-of-sample scenarios with our strategic policy's optimal stack. The third column presents the average profit results for the fixed policy in which the consumer targets a given quantity of consumption. We have adjusted this experiment for the different levels of  $u$ , thereby the fixed consumption level is set to be higher in the experiments with greater  $u$  values, and lower for smaller  $u$  values. The fourth column presents the average profit of the clairvoyant policy when solved for each out-of-sample scenario. The fifth column shows the increase in the profit when using our proposed policy, versus the fixed policy (the policy that is used in practice by NZAS). The last column presents the percentage of clairvoyant policy's profit that is recovered by our proposed stochastic out-of-sample policy. Moreover, Fig. 15 lays out the standard box-and-whisker plots corresponding to winter peak profit values for different levels of  $u$ .

Table 8: Policy performance – winter peak.

$u$	Average profit (\$)			Profit increase	% of clairvoyant
	Optimal Stack	Fixed Quantity	Clairvoyant		
30	3405	3245	4313	4.9%	78.9%
50	10209	7283	11004	40.1%	92.7%
70	18474	13438	19783	37.4%	93.3%
90	27238	20006	29655	36.1%	91.8%
110	35993	27529	40895	30.7%	88.0%
Average	19064	14300	21130	29.8%	88.9%

In addition to peak trading periods, we also simulated policies for off-peak trading periods in winters 2016 and 2017. Table 9 outlines the average results of 300 simulations that implemented the optimal policies for peak and off-peak prices.

Table 9: Winter policy performance.

TP Type	Average profit (\$)			Profit increase	% of clairvoyant
	Optimal Stack	Fixed	Clairvoyant		
Winter peak	27238	20006	29655	36.1%	91.8%
Winter off-peak	32395	25343	35301	27.8%	91.7%

In order to extend the simulation to a broader range of trading periods we have run experiments on 2018/2019 summer, which had a series of high prices due to lake levels running low towards the end of summer. We have sampled scenarios from weekdays in December 2017 and January 2018, separately for summer afternoon peak (1pm–6pm) and early morning off-peak (3am–6am) trading periods.

Table 10: Summer policy performance

TP Type	Average profit (\$)			profit increase	clairvoyant cover
	Optimal Stack	Fixed	Clairvoyant		
Summer peak	15735	4807	19484	227.3%	80.7%
Summer off-peak	28111	18147	36471	54.9%	77.0%

<sup>6</sup> The marginal value of electricity for NZAS may change over time as it is affected by exogenous parameters such as the global price of aluminum, government policies, etc.



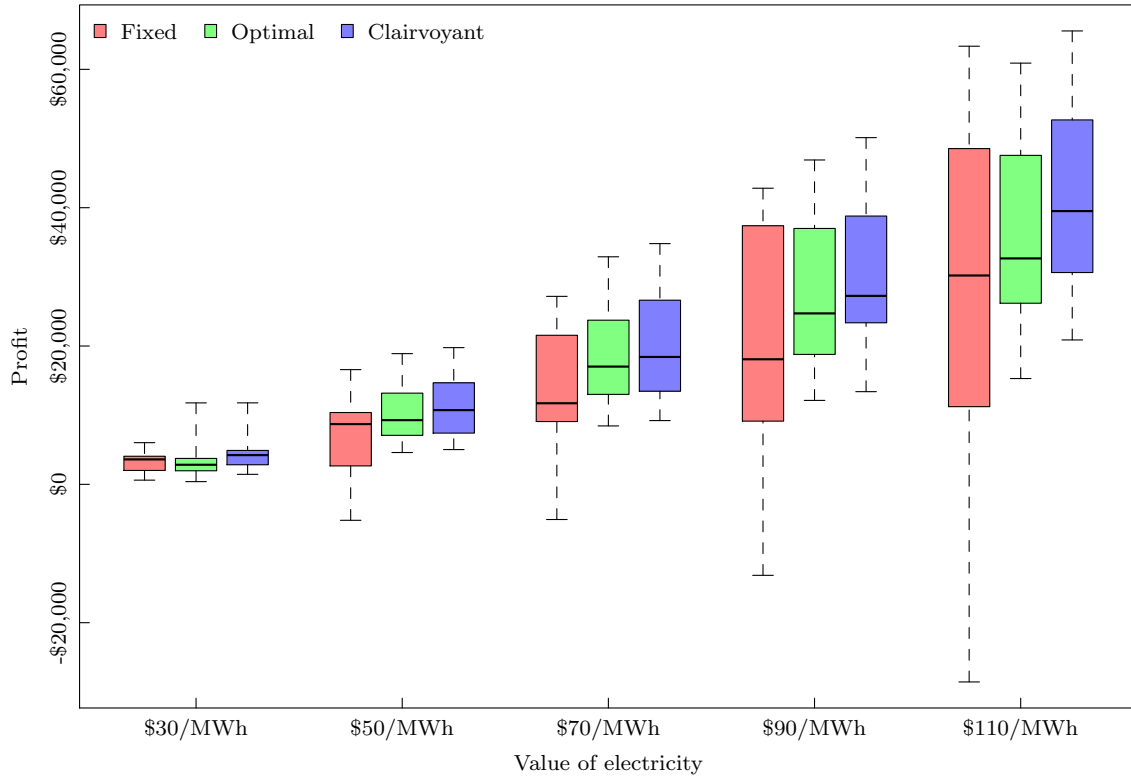


Fig. 15: Winter peak profit for different values of electricity ( $u$ ).

In this experiment, the sampled trading periods (from summer 2017/2018) have a higher average price than that of the time periods from same time of year in the previous years. The reason we picked this particular set of trading periods is that there had been an anticipation of high prices given the dry summer and low reservoir levels. Hence such signals could have been used by the major consumers to change their consumption plans in order to prevent high prices. In this experiment we have used a mid-February week's trading periods to represent our out-of-sample scenarios, in order to show the effect of incorporating our proposed policy while taking into account the anticipation of low lake levels. In Table 10 we compare the performance of our optimal stacks with the current policy employed by NZAS (which disregards the price signals). According to the simulation results, our proposed policy can lead to more than twice as much profit on average, when compared with the fixed policy, in peak trading periods.

## 6 Conclusions

In this paper we have considered major consumers whose demand for energy and ability to provide ILR affect the market. By explicitly modelling a consumer's impact on prices, they can anticipate how their actions can lead to lower costs and therefore higher profit. In order to determine the optimal energy bids and ILR offers for such strategic major consumers, we lay out a bi-level optimization model that has the co-optimized OPF problem embedded inside. One of the key attributes of this model is its capturing of the link between electricity consumption and ILR; this yields insights such as that a major consumer may choose to consume more electricity, in order to benefit from further participation in reserve market.

In order to address uncertainty, we presented a stochastic model that optimizes over a set of scenarios, delivering optimal admissible ILR offer and consumption bid curves for a large consumer of electricity. This is a bi-level optimization problem, however, due to stochasticity and the resulting monotonicity constraints, using the standard MIP reformulation using big-M constraints quickly becomes intractable. In order to reduce the complexity and solution time, we introduced a novel decomposition method to enhance our formulation. The decomposition has enabled us to apply our

method for a major consumer in the NZEM, and solve it over a set of 20 scenarios, which resulted in an approximately 30% increase in expected profit, over a fixed consumption approach.

Our model has provided significant intuition for a major consumer's consumption and reserve offer strategy for one trading period. However, a large consumer also can shift consumption of electricity by utilizing flexibility in its production schedule. The consumer's problem, over a sensible time horizon, is the subject of future work.

## Appendix

### A Bi-parametric sensitivity analysis reformulation algorithm

Suppose that we have a linear program [LP] in standard computational form:

$$\begin{aligned} \text{[LP]} \quad & \min && c^T x \\ & \text{s.t.} && Ax = b \quad [\pi] \\ & && x \geq 0, \end{aligned}$$

where we denote  $b_i$  as the  $i^{\text{th}}$  component of the right-hand side vector  $b$ , and  $\pi$  as the optimal dual vector. We aim to find  $(\pi_1, \pi_2)$  as a function of the right-hand sides  $(b_1, b_2)$ . In order to define this function, we use the following algorithm:

#### Step 1: Set Initial Values

Set feasible initial values of  $b_1$  and  $b_2$  in [LP]. Without loss of generality, we set  $b_1 = b_2 = 0$ . Define set  $\mathcal{R} = \{\}$  as the set of all regions. Define  $\mathcal{R}_r = \{\}$  a subset of  $\mathcal{R}$ , as the set of all extreme points in region  $r$ . Set  $r = 1$ .

#### Step 2: Set Initial Optimal Basis

Retrieve the optimal basis for [LP] given the values of  $b_1$  and  $b_2$ . We store the basis data for the vector of basic variables  $x_B$ . Note that:

$$\text{Given } Bx_B = b \implies x_B = B^{-1}b \qquad \text{Since } x_B \geq 0 \implies B^{-1}b \geq 0.$$

#### Step 3: Define [S-LP]

$$\begin{aligned} \text{[S-LP]} \quad & \max_{b_1, b_2} && c_1 b_1 + c_2 b_2 \\ & \text{s.t.} && B_{i,1}^{-1} b_1 + B_{i,2}^{-1} b_2 \geq 0 \qquad \forall i \in \mathcal{I} \end{aligned}$$

Here  $B_{i,1}^{-1}$  is the first column of the  $i^{\text{th}}$  row of  $B$  matrix, and  $\mathcal{I}$  is the set of all rows in  $B$  matrix.

#### Step 4: Set initial $c$ values

At the first iteration we set  $c_1 = 1$  and  $c_2 = -\infty$ .

#### Step 5: Solve [S-LP]

Solve [S-LP] and add the pair of optimal solution values  $(b_1^*, b_2^*)$  to the set  $\mathcal{R}_i$ .

#### Step 6: Get objective coefficient sensitivity information

Using sensitivity analysis find largest objective coefficient value ( $c_2$ ) at which the current optimal basis would remain optimal. Store it as  $c_2'$ .

#### Step 7: Change $c_2$ coefficient

- If  $c_2' \leq \infty$ , set  $c_2 = c_2' + \epsilon$  in [S-LP] and go to step 5.
- If  $c_2' = \infty$  and  $c_1 = 1$ , go to step 8.
- If  $c_2' = \infty$  and  $c_1 = -1$ , go to step 9.

*Step 8: Change  $c_1$  coefficient*

Set  $c_1 = -1$ , and go to step 5.

*Step 9: Make seed points*

- Define seed set  $\mathcal{S} = \{\}$ .
- Find the convex hull formed by the pairs in  $\mathcal{R}_i$ .
- Find an exterior point for each edge, and add the pairs to  $\mathcal{S}$  as  $(b_1^s, b_2^s)$ .
- Set  $i = i + 1$ .

*Step 10: Use seed points*

- If  $\mathcal{S} \neq \emptyset$ , choose a pair  $(b_1^s, b_2^s)$  from  $\mathcal{S}$ . Set  $b_1 = b_1^s$  and  $b_2 = b_2^s$ . Remove  $(b_1^s, b_2^s)$  from  $\mathcal{S}$ , and go to step 2.
- if  $\mathcal{S} = \emptyset$ , go to step 11.

*Step 11: Make vertical regions*

In order to allow for the optimal solution to lie on the vertical tranches of the residual stack, we add vertical regions to the set of regions  $\mathcal{R}$  at this step.

1. Set  $i = 1$ , and  $\mathcal{V} = \{\}$ .
2. For each edge in  $\mathcal{R}_i$  take the corresponding pairs of  $(y^d, \pi_i^d)$  and  $(y^r, \pi_i^r)$  for the two extreme points on the edge. Store them as point 1 and 2, (e.g.  $y^{d1}, y^{d2}$ ).
3. Find the adjacent region  $j$  to the chosen edge, and store  $\pi_j^d$  and  $\pi_j^r$ .
4. Set  $\mathcal{Q} = \{\{(y^{d1}, \pi_i^d), (y^{r1}, \pi_i^r)\}, \{(y^{d2}, \pi_i^d), (y^{r2}, \pi_i^r)\}, \{(y^{d1}, \pi_j^d), (y^{r1}, \pi_j^r)\}, \{(y^{d2}, \pi_j^d), (y^{r2}, \pi_j^r)\}\}$ .
5. If  $\mathcal{Q} \notin \mathcal{V}$ , add  $\mathcal{Q}$  to  $\mathcal{V}$ .
6. Set  $i = i + 1$
7. If  $i \leq |\mathcal{R}|$ , go back to line 2.
8. If  $i = |\mathcal{R}|$ , set  $\mathcal{R} = \mathcal{R} \cup \mathcal{V}$ .

## B Scenario selection examples

In this appendix we present examples to illustrate our choice of a scenario set regarding the similarity of scenarios. First, we lay out an example, in which we use the full-scale network's historical data. Suppose  $\Omega_1$  and  $\Omega_2$  are two scenario sets, and  $|\Omega_1| = |\Omega_2| = 6$ . Here  $\Omega_1$  consists of similar scenarios, all picked from a morning peak on a single day, in winter 2016. On the other hand,  $\Omega_2$  consists of semi-similar scenarios, chosen from morning peaks of two days in winter 2016 and 2017. We solve  $[\alpha\text{-MIP}]$  for both sets and obtain the optimal expected actions for each scenario set. Figure 16 shows the optimal stacks for the two sample sets, here S1 and S2 correspond to the optimal bid stacks from optimizing against  $\Omega_1$  and  $\Omega_2$  respectively.

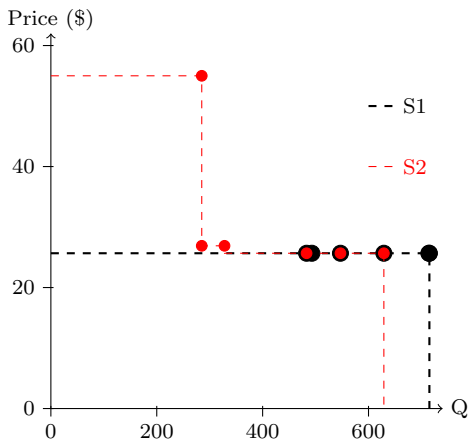


Fig. 16: Sample set comparison

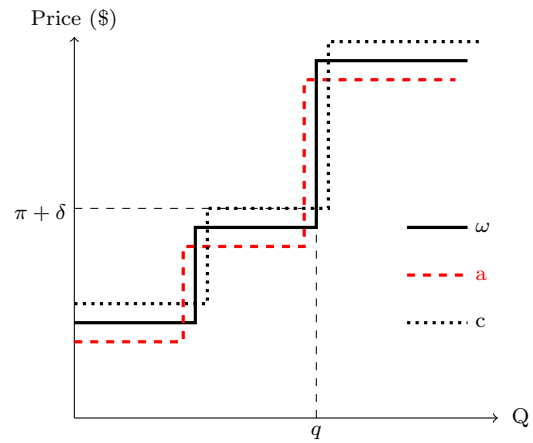


Fig. 17: Similar scenarios

As shown in figure 16, S2 consists of three steps, that enable it to respond to different types of time periods. The three mutual scenarios in the two scenarios sets, have the same optimal consumption - price pairs in the two

stacks (the overlapped points), and results in equal in-sample profit for the mutual points. However, the diversity of scenarios in  $\Omega_2$ , enhances the performance of S2 for out-of-sample scenarios. Table 11 reports on each stack's profit when simulated over 100 out-of-sample scenarios.

Table 11: Out-of-sample performance comparison

Stack	Profit (\$)		
	Average	Min.	Max.
S1	15707	10109	21571
S2	17841	12238	21637

In the second part of this appendix, we use a generic example to parametrically calculate the impacts of scenario selection. Suppose we have scenario  $\omega$ , with the residual supply stack shown with black line in Figure 17, and with the optimal consumption-price pair  $(q, \pi)$ . We introduce new scenarios (a-d), whose residual stack deviates from that of  $\omega$  with distance  $\delta$  in each dimension. For the sake of simplicity we only show 2 out of 4 stacks (a and c) in Fig. 17. Here scenario a's residual stack is shown in red, and its optimal consumption-price pair is  $(q - \delta, \pi - \delta)$ , and that of scenario c is  $(q + \delta, \pi + \delta)$ . Similarly, scenario b and d have the optimal consumption-price pairs  $(q - \delta, \pi + \delta)$  and  $(q + \delta, \pi - \delta)$ , respectively. If we solve  $[\alpha\text{-MIP}]$  for  $\Omega = \{\omega\}$ , the optimal stack will have one step with the point  $(q, \pi)$ . However, in order to cover the optimal consumption for the scenarios whose prices are higher with  $\delta$  divergence from  $\pi$ , we draw the optimal stack based on the quantity-price pair  $(q, \pi + \delta)$ , which is presented with the dashed gray line in Figure 17. We call this stack  $\omega$ -stack.

In table 12 we compare using the clairvoyant policy versus the optimal stack generated with  $\Omega$ , for all scenarios  $\omega$  and a-d. Here the difference between the clairvoyant policy and  $\omega$ -stack, depends on  $\delta$ . Note that when we set  $\delta \ll q$ , the difference in profit becomes very small. This implies that adding similar scenarios to the scenario set, has little contribution to the performance of the actions, but makes the problem much harder to solve. Therefore, it would be beneficial to pick a representative scenario in  $\Omega$ , instead of including all similar scenarios.

Table 12: Profit vs policy

Scenario	Clairvoyant	$\omega$ -stack	Difference
$\omega$	$(u - \pi)q$	$(u - \pi - \delta)q$	$\delta q$
a	$(u - \pi + \delta)(q - \delta)$	$(u - \pi - \delta)(q - \delta)$	$2\delta(q - \delta)$
b	$(u - \pi - \delta)(q - \delta)$	$(u - \pi - \delta)(q - \delta)$	0
c	$(u - \pi - \delta)(q + \delta)$	$(u - \pi - \delta)q$	$\delta(u - \pi - \delta)$
d	$(u - \pi + \delta)(q + \delta)$	$(u - \pi + \delta)q$	$\delta(u - \pi + \delta)$

In this example we showed that the more a scenario is similar to the existing scenarios in the sample set, the less adding that scenario (to the sample set) will improve the performance of the optimal action. Hence, we construct our random sets  $\Omega$ , while ensuring two similar scenarios are not picked. However, the information on the number of occurrences of similar scenarios will be incorporated in the probability of their representative scenario.

## References

1. P. Cramton, S. Stoft, A capacity market that makes sense, *The Electricity Journal* **18**(7), 43 (2005)
2. M.H. Albadi, E. El-Saadany, A summary of demand response in electricity markets, *Electric power systems research* **78**(11), 1989 (2008)
3. N. Li, L. Chen, S.H. Low, in *Power and Energy Society General Meeting, 2011 IEEE* (IEEE, 2011), pp. 1-8
4. H. Sæle, O.S. Grande, Demand response from household customers: experiences from a pilot study in norway, *Smart Grid, IEEE Transactions on* **2**(1), 102 (2011)
5. K.M. Tsui, S.C. Chan, Demand response optimization for smart home scheduling under real-time pricing, *Smart Grid, IEEE Transactions on* **3**(4), 1812 (2012)
6. P. Aketi, S. Sen, Modeling demand response and economic impact of advanced and smart metering, *Energy Systems* **5**(3), 583 (2014)
7. P.C. Del Granado, S.W. Wallace, Z. Pang, The value of electricity storage in domestic homes: a smart grid perspective, *Energy Systems* **5**(2), 211 (2014)
8. D.W. Caves, J.A. Herriges, Optimal dispatch of interruptible and curtailable service options, *Operations Research* **40**(1), 104 (1992)
9. S. Majumdar, D. Chattopadhyay, J. Parikh, Interruptible load management using optimal power flow analysis, *IEEE Transactions on Power Systems* **11**(2), 715 (1996)
10. K. Bhattacharya, et al., Competitive framework for procurement of interruptible load services, *IEEE Transactions on Power systems* **18**(2), 889 (2003)
11. C.L. Su, D. Kirschen, Quantifying the effect of demand response on electricity markets, *IEEE Transactions on Power Systems* **24**(3), 1199 (2009)

12. D.S. Kirschen, Demand-side view of electricity markets, *IEEE Transactions on Power Systems* **18**(2), 520 (2003)
13. S.H. Madaeni, R. Sioshansi, The impacts of stochastic programming and demand response on wind integration, *Energy Systems* **4**(2), 109 (2013)
14. EPA. Electricity Customers. [https://www.eia.gov/electricity/annual/html/epa\\_01\\_02.html](https://www.eia.gov/electricity/annual/html/epa_01_02.html). [Online; accessed 16-Jan-2018]
15. Electricity Authority. Electricity in New Zealand. <https://www.ea.govt.nz/about-us/media-and-publications/electricity-nz/>. [Online; accessed 24-Jan-2018]
16. A.J. Conejo, J. Contreras, J.M. Arroyo, S. De la Torre, Optimal response of an oligopolistic generating company to a competitive pool-based electric power market, *Power Systems, IEEE Transactions on* **17**(2), 424 (2002)
17. S.J. Kazempour, A.J. Conejo, C. Ruiz, Strategic bidding for a large consumer, *IEEE Transactions on Power Systems* **30**(2), 848 (2015)
18. A. Daraeepour, S.J. Kazempour, D. Patiño-Echeverri, A.J. Conejo, Strategic demand-side response to wind power integration, *IEEE Transactions on Power Systems* **31**(5), 3495 (2016)
19. M. Fisher, J. Apt, F. Sowell, The economics of commercial demand response for spinning reserve, *Energy Systems* **9**(1), 3 (2018)
20. N. Cleland, G. Zakeri, G. Pritchard, B. Young, Boomer-consumer: a model for load consumption and reserve offers in reserve constrained electricity markets, *Computational Management Science* **12**(4), 519 (2015)
21. N. Cleland, G. Zakeri, G. Pritchard, B. Young, in *Computational Management Science* (Springer, 2016), pp. 23–30
22. E. Ela, M. Milligan, B. Kirby, Operating reserves and variable generation, *Contract* **303**, 275 (2011)
23. J.F. Ellison, L.S. Tesfatsion, V.W. Loose, R.H. Byrne, Project report: A survey of operating reserve markets in us iso/rto-managed electric energy regions, Sandia Natl Labs Publications. Available Online: [http://www.sandia.gov/ess/publications/SAND2012\\_1000](http://www.sandia.gov/ess/publications/SAND2012_1000) (2012)
24. Transpower. Under Frequency Event Reports. <https://www.transpower.co.nz/system-operator/key-documents/under-frequency-event-reports>. [Online; accessed 1-Oct-2018]
25. Electricity Authority. Wholesale Datasets. <https://www.emi.ea.govt.nz/Wholesale/Datasets>. [Online; accessed 17-November-2017]
26. J. Fortuny-Amat, B. McCarl, A representation and economic interpretation of a two-level programming problem, *Journal of the Operational Research Society* pp. 783–792 (1981)
27. B.F. Hobbs, C.B. Metzler, J.S. Pang, Strategic gaming analysis for electric power systems: An mpec approach, *IEEE transactions on power systems* **15**(2), 638 (2000)
28. M.V. Pereira, S. Granville, M.H. Fampa, R. Dix, L.A. Barroso, Strategic bidding under uncertainty: a binary expansion approach, *IEEE Transactions on Power Systems* **20**(1), 180 (2005)
29. C. Ruiz, A.J. Conejo, Pool strategy of a producer with endogenous formation of locational marginal prices, *IEEE Transactions on Power Systems* **24**(4), 1855 (2009)
30. A.G. Bakirtzis, N.P. Ziogos, A.C. Tellidou, G.A. Bakirtzis, Electricity producer offering strategies in day-ahead energy market with step-wise offers, *IEEE Transactions on Power Systems* **22**(4), 1804 (2007)
31. M.A.M. Paul D. Klemperer, Supply function equilibria in oligopoly under uncertainty, *Econometrica* **57**(6), 1243 (1989). URL <http://www.jstor.org/stable/1913707>